

Quark-Gluon Plasma Fireball

Salah Hamieh, Jean Letessier and Johann Rafelski

Department of Physics, University of Arizona, Tucson, AZ 85721
and

Laboratoire de Physique Théorique et Hautes Energies
Université Paris 7, 2 place Jussieu, F-75251 Cedex 05.
(June 7, 2000)

Lattice-QCD results provide an opportunity to model, and extrapolate to finite baryon density, the properties of the quark-gluon plasma (QGP). Upon fixing the scale of the thermal coupling constant and vacuum energy to the lattice data, the properties of resulting QGP equations of state (EoS) are developed. We show that the physical properties of the dense matter reball formed in heavy ion collision experiments at CERN-SPS are well described by the QGP-EoS we presented. We also estimate the properties of the reball as it is formed just after nuclear collision is completed, and argue that QGP formation must be expected down to 40 A GeV central Pb-Pb interactions.

PACS: 12.38Mh, 12.40Ee, 25.75.-q

I. INTRODUCTION

It is believed today that a new state of matter has been formed in relativistic nuclear collisions at CERN [1]. The existence of a novel non-nuclear high temperature phase of elementary hadron matter, consisting of deconfined quarks and gluons, arises from the current knowledge about quantum chromodynamics (QCD), the theory of strong interaction. At issue is today if the new phase of matter observed at CERN is indeed this so called quark-gluon plasma (QGP) phase. One of the ways to test, and possibly falsify, the QGP hypothesis is to consider if the expected properties of the QGP indeed agree with experimental data which have been at the heart of the CERN announcement. Our main aim is thus to relate the properties of the QGP phase, modeled to agree with the lattice QCD calculations [2], to the hadronic particle spectra and abundances observed.

As seen in many experimental results [1], which we will not restate here in further detail, in these high energy nuclear collisions a localized dense and hot matter reball is formed. We address here hadron and strange hadron production at the equivalent center of momentum reaction energy $E_{CM} = 8.6$ GeV per baryon in Pb-Pb reactions. The observational output of all experiments are particle abundances and particle spectra. In our earlier analysis of hadronic, and in particular strange hadronic particles [3,4], we have obtained diverse physical properties of the source, such as energy per baryon content $E=b$, entropy per baryon content $S=b$, temperature at which abundances are produced (chemical freeze out temperature) T_f , baryo-chemical potential μ_b at the freeze-out point, collective velocity of the matter emitting these particles v_c , and last, not least, strangeness content per baryon $s=b$. Clearly, these properties must be consistent with equations of state of the source, and thus our current work aims to verify this consistency of a QGP source by checking if these prior results agree with the QGP physical properties we derive. We have already

shown previously that the strangeness yield is following the predicted QGP yield.

An important dynamical aspect of our earlier analysis [3], is an apparently sudden disintegration and hadronization of the new form of matter reball into the final state hadrons. This is a priori not very surprising, since a reball formed in these collisions explodes, driven by internal compression pressure. We show that indeed the hadronization temperature we found corresponds to a deeply supercooled state which can be subject to mechanical instability [5], and thus disintegrate in a violent and sudden fashion. A consequence of the sudden break up is that akin to the situation found in the theoretical description of the early universe all particle abundances should be allowed to be in chemical non-equilibrium. Our analysis accounts in full for this important fact [3]. For an appropriate criticism of the chemical equilibrium description approaches and a list of related work we refer the reader to work of Biro [6].

In the next section, we address the thermal QCD interaction coupling g_s we will use. In section III, we define the equations of state and the parameters of our approach and explore which is the best scheme for the extrapolation of the lattice data. In section IV, we present properties of the QGP phase, relevant both to the study of the freeze-out conditions, and the study of the initial conditions reached in the collision. We present and discuss the comparison of the properties of the exploding reball with those measured by means of hadron production in section V. Our conclusions follow in section VI.

II. QCD INTERACTIONS IN PLASMA

The energy domain in which we explore diverse properties of dense strongly interacting matter is barely above the scale 1 GeV and thus, in our consideration, an important input is the scale dependence of the QCD coupling constant, $g_s(\mu)$, which we obtain solving

$$\frac{d\alpha_s}{d\ln L} = b_0 \alpha_s^2 + b_1 \alpha_s^3 + \dots + \beta_2^{\text{pert}} : \quad (1)$$

β_2^{pert} is the beta-function of the renormalization group in two loop approximation, and

$$b_0 = \frac{11 - 2n_f}{2}; \quad b_1 = \frac{51 - 19n_f}{4} :$$

β_2^{pert} does not depend on the renormalization scheme, and solutions of Eq.(1) differ from higher order renormalization scheme dependent results by less than the error introduced by the experimental uncertainty in the measured value of $\alpha_s(\mu = M_Z) = 0.118 \pm 0.001 \pm 0.0016$. When solving Eq.(1) with this initial condition, we cross several avormass thresholds and thus $n_f(\mu)$ is not a constant in the interval $\mu \in (1; 100) \text{ GeV}$. Any error made when not properly accounting for n_f dependence on μ accumulates in the solution of Eq.(1). In consequence, a popular approximate analytic solution shown as function of T , as dotted line in figure 1,

$$\alpha_s(\mu) \approx \frac{2}{b_0 L} \left[1 - \frac{2b_1}{b_0^2} \frac{\ln L}{L} \right]; \quad L = \ln(\mu^2/\Lambda^2); \quad (2)$$

with $\Lambda = 0.15 \text{ GeV}$ and $n_f = 3$, is not precise enough compared to the exact 2-loop numerical solution.

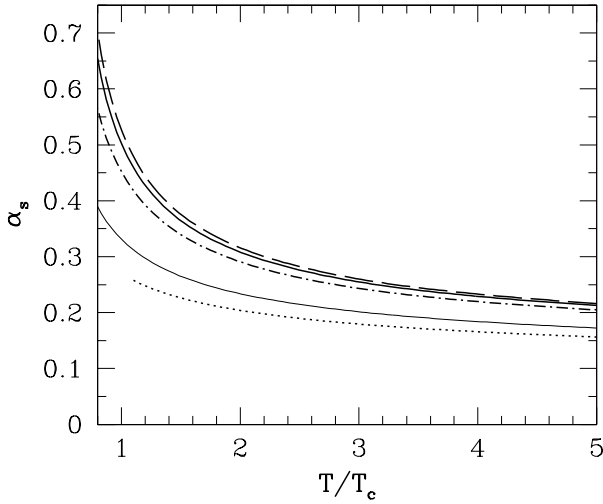


FIG. 1. $\alpha_s(2T)$ for $T_c = 0.16 \text{ GeV}$. Dashed line: $\alpha_s(M_Z) = 0.119$; solid line = 0.118 ; dot-dashed line = 0.1156 . Dotted line: approximate 2-loop solution given in Eq.(2). Thin solid line: same as dotted, but extrapolating with $n_f = 5$ to $\alpha_s(M_Z) = 0.118$.

We show the numerical solution for $\alpha_s(\mu)$ in figure 1, setting

$$\mu = 2T = T = T_c; \quad \Lambda = 1 \text{ GeV} :$$

where the solid line corresponds to $\alpha_s(\mu = M_Z) = 0.118$, bounded by the experimental uncertainty [7]. We observe that the expansion parameter of thermal QCD is relatively small, $\alpha_s < 0.25$, which makes the following

discussion possible. The difference between the dotted line and the exact result, in figure 1, is very relevant and has been at the origin of considerable confusion regarding the behavior of the interacting hot quark-gluon gas [8]. Since the lattice work chooses the value of T_c to match the string tension, use of false α_s is physically inconsistent.

We stress that the analytical function Eq.(2) is in fact a very good solution of Eq.(1). For $\mu = 0.225 \text{ GeV}$ and $n_f = 5$, it agrees with numerical result for the entire range, $M_Z = 92 \text{ GeV} > \mu > M_B \approx 4.5 \text{ GeV}$, in which $n_f = \text{Const.}$, here M_B is the bottom quark mass. However, these were not the parameters considered in the thermal QCD work [9][12], and, moreover, the region of interest for the QGP equations of state we explore is $1 \text{ GeV} < \mu < M_B$, where n_f varies. The thin solid line, in figure 1, shows the behavior of the analytical solution with $n_f = 5$ kept constant, and for $\mu = 0.225 \text{ GeV}$ which assures the boundary value $\alpha_s(M_Z) = 0.118$.

III. THE QUARK-GLUON LIQUID

We now can define the quark-gluon liquid model which describes well the properties of QGP determined by lattice-QCD method.

1. To relate the QCD scale to the temperature $T = 1/\beta$ we use for the scale [13]:

$$\mu = 2^{-1} \frac{r}{1 + \frac{1}{2} \ln^2 \frac{r}{q}} = 2^{-1} \frac{q}{(T)^2 + \frac{2}{q}} : \quad (3)$$

This extension to finite chemical potential q , or equivalently quark fugacity $q = \exp(\mu/T)$, is motivated by the form of plasma frequency entering the computation of the vacuum polarization function [14].

2. To reproduce the lattice results available at $q = 0$ [2], we need to introduce, in the domain of freely mobile quarks and gluons, a finite vacuum energy density [8]:

$$B = 0.19 \frac{\text{GeV}^4}{\text{fm}^3} :$$

This also implies, by virtue of relativistic invariance, that there must be a (negative) associated pressure acting on the surface of this volume, aiming to reduce the size of the deconfined region. These two properties of the vacuum follow consistently from the vacuum partition function:

$$\ln Z_{\text{vac}} = -BV : \quad (4)$$

3. The partition function of the quark-gluon liquid comprises interacting quarks and gluons [15], and the vacuum B-term,

$$\frac{T}{V} \ln Z_{\text{QGP}} = P_{\text{QGP}} = B + \frac{8}{45} c_1 (T)^4 + \frac{n_f}{15} \frac{7}{4} c_2 (T)^4 + \frac{15}{2} c_3 \frac{2}{q} (T)^2 + \frac{1}{2} \frac{4}{q} ; \quad (5)$$

where:

$$c_1 = 1 \frac{15}{4} s + \quad ;$$

$$c_2 = 1 \frac{50}{21} s + \quad ; \quad c_3 = c_1 \frac{2}{s} + \quad :$$

Beyond the leading term, the series expansion, in terms of the QCD-coupling constant g , has been carried out to order $(g=4)^5 = (s=)^{5=2}=32$ [10], yet the higher order terms do not appear to lead to a convergent result for the range of temperatures of interest to us [12]. It is not uncommon to encounter in a perturbative expansion a semi-convergent series. The issue then is how to establish a workable scheme. Exploring the effect of the interactions [8], one finds, using just the lowest terms Eq. (6) in Eq. (5), that the results obtained numerically using lattice QCD [2], are very well reproduced.

In figure 2, the 'experimental' values are from numerical lattice simulations of $P=T^4$ [2]. For practical reasons the lattice results for massless 2 and 3-avors were obtained with $m=T=0.4$, which reduces the particle numbers by 2%, and this effect is allowed for in the quark-gluon liquid lines (two avors: dashed, three avors: dotted) in figure 2. In the case 2+1 avors, a renormalized strange quark mass $m_s=T=1.7$, which leads to a ~50% reduction in strange quark number was used, the lattice input has been $m_s^0=T=1$. When reporting the properties of the QGP liquid, we will set $n_f=2.5$, assuming that strangeness is fully chemically equilibrated, unless otherwise noted.

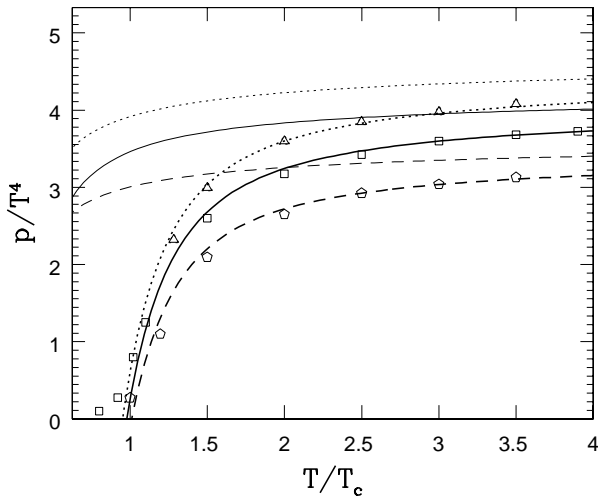


FIG. 2. Lattice-QCD results [2] for $P=T^4$ at $q=1$, compared with our quark-gluon liquid model (thick lines) and lowest order perturbative QCD using approximate s , Eq. (2) (thin lines used in prior work [9][12]); dotted line 3 avors, solid line 2+1 avors, and dashed line 2 avors.

The thin lines, in figure 2, correspond to the previously reported results for a quark-gluon gas [12], with first order QCD correction introduced using an approximate value of $s(\cdot)$, Eq. (2), and without the vacuum

pressure term. For $T > 2T_c$, the disagreement is an artifact of the approximation used for s .

- (6) Lattice results were also informally reported [1] for the energy density with $n_f=3$, and are shown in figure 3, upper 'experimental' points. The energy density,

$$\epsilon_{QGP} = \frac{\partial \ln Z_{QGP}(\cdot; \cdot)}{\partial V} ; \quad (7)$$

is sensitive to the slope of the partition function. We show, in figure 3, the energy density and pressure for two extreme theoretical approaches: the solid lines are for the model we described above ($\mu=2T; B=0.19 \text{ GeV}/\text{fm}^3$), the dotted lines are obtained in the thermal expansion, including all, up to fifth order, scale dependent terms obtained by Zhai and Kastening [10], and choosing the scale $\mu=2.6T$ in free energy and in the coupling constant, so the result reproduces the pressure well (bottom dotted line in figure 3).

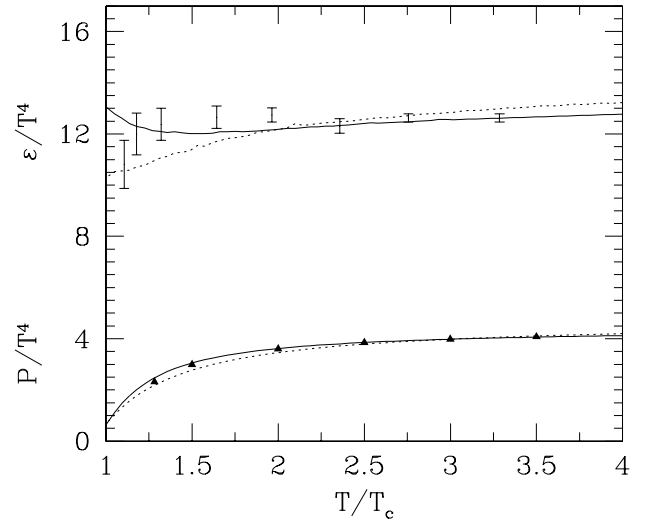


FIG. 3. Top: informal lattice-QCD results [1] for $\mu=T^4$ at $q=1$, compared with our quark-gluon liquid model (solid line). Dotted line is an alternative approach in which all terms in partition function are summed as given in [10] and the scale is set at $\mu=2.6T$. Bottom: published lattice pressure results [2] compared to the two approaches: solid line first order with the bag constant, dotted line 5th order with $\mu=2.6T$.

We see, in upper portion of figure 3, a clear difference in the energy density between these two theoretical approaches, chosen to reproduce the pressure well. In particular, close inspection of these results shows that the 5th order energy density at high T disagrees with the lattice data, where these are very precise. Also we note that near to $T \approx 1.5T_c$, the solid line is better describing the pressure. Thus aside of the elegance of using the Matsubara frequency $2T$ as the scale, there is the fact that this very simple approach adequately describes both pressure and energy density, which supports our belief that we have found a good opportunity for the extrapolation of the QGP properties to finite baryon density. The

reader should be aware that the quantities we show are all divided by a huge factor, T^4 and thus any differences between our model and lattice results are greatly amplified. In fact, in absolute terms, the model we now adopt for further study reproduces the lattice results well.

Before proceeding, we stress that we could not test if the coefficient c_3 , Eq. (6), describes well the behavior of the partition function for finite chemical potentials, as such results are not available. By using this term, we rely on the expansion in μ_b as implied by Eq. (5). This, in fact, is a third reason for us to prefer the simpler approach, since the expansion of Zhai and Kastening [10], was only computed for a vanishing chemical potential.

IV. PROPERTIES OF QGP-LIQUID

We are now ready to explore the physical properties of the quark-gluon liquid. The energy density is obtained from Eq. (5), recalling that the scale of the interaction is given by Eq. (3):

$$P_{QGP} = 4B + 3P_{QGP} + A; \quad (8)$$

$$A = (b_0 \frac{2}{s} + b_1 \frac{3}{s}) \frac{2}{3} T^4 + \frac{n_f 5}{18} T^4 + \frac{n_f}{2} \frac{2}{q} T^2 + \frac{1}{2} \frac{4}{q} : \quad (9)$$

A convenient way to obtain entropy and baryon density uses the thermodynamic potential F :

$$\frac{F(T; q; V)}{V} = \frac{T}{V} \ln Z(\mu_b; q; V)_{QGP} = -P_{QGP}; \quad (10)$$

The entropy density is:

$$s_{QGP} = \frac{dF}{V dT} = \frac{32}{45} c_1 T^3 + \frac{n_f 7}{15} c_2 T^3 + n_f c_3 \frac{2}{q} T + A \frac{2T}{2T^2 + \frac{2}{q}}; \quad (11)$$

Noting that baryon density is 1/3 of quark density, we have:

$$B = \frac{1}{3} \frac{dF}{V d\mu_b};$$

$$= \frac{n_f}{3} c_3 \frac{2}{q} T^2 + \frac{1}{2} \frac{3}{q} + \frac{1}{3} A \frac{q}{2T^2 + \frac{2}{q}}; \quad (12)$$

We show properties of the quark-gluon liquid in a wider range of parameters in figure 4. We study the properties at fixed entropy per baryon $S=b$ since an isolated ideal particle reball would evolve at a fixed $S=b$. We consider the range $S=b = 10$ (at left for the top panel, baryochemical potential μ_b , and middle panel baryon density n/n_0 , here $n_0 = 0.16 \text{ fm}^{-3}$, and bottom left for the energy per baryon E/b) in step of 5 units, up to maximum of $S=b = 60$. The highlighted curve, in figure 4, is for

the value $S=b = 40$, which is the trajectory of the reball made in Pb-Pb interactions at the projectile energy 160A GeV. The dotted line at the minimum of $E/b_{S=b}$ is where the vacuum and quark-gluon gas pressure balance. This is the equilibrium point and indeed the energy per baryon does have a relative minimum there. We note that unlike the case for an ideal quark-gluon gas, the lines of fixed $S=b$, seen in the top panel of figure 4 are not corresponding to $\mu_b = T = \text{Const.}$, though for large T and small μ_b they do show this asymptotic behavior.

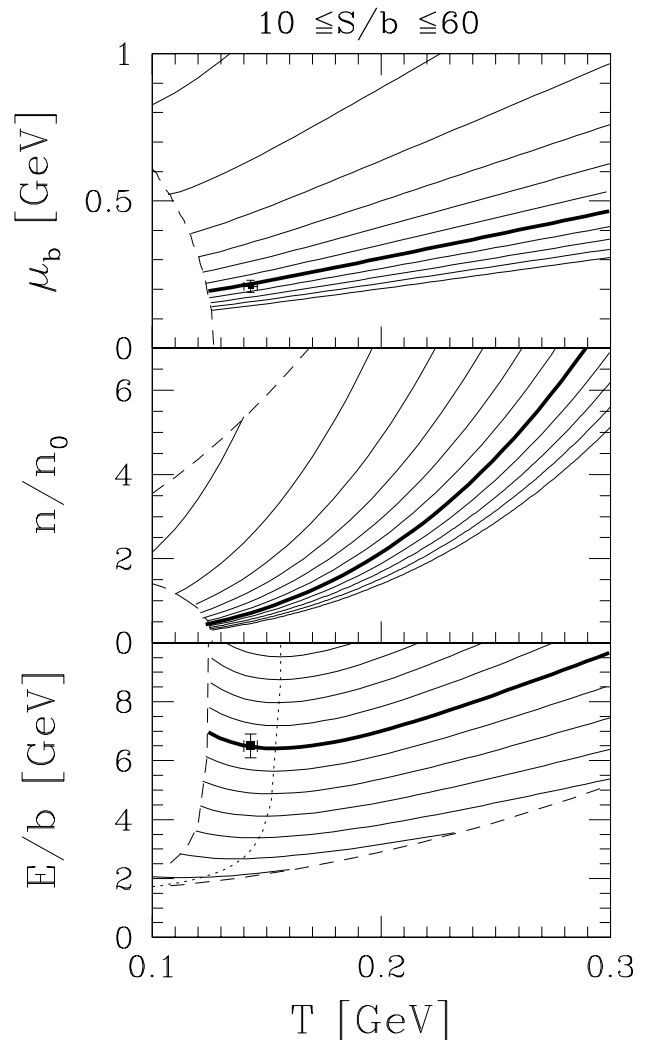


FIG. 4. From top to bottom: μ_b ; n/n_0 and E/b ; lines shown correspond to fixed entropy per baryon $S=b = 10$ to 60 by step of 5 (left to right). Limits: energy density $\epsilon_{q/g} = 0.5 \text{ GeV}/\text{fm}^3$ and baryochemical potential $\mu_b = 1 \text{ GeV}$. The experimental points denote chemical freeze-out analysis result [3], see section V.

The trajectories at fixed energy per baryon E/b are shown in the $T - \mu_b$ plane in figure 5, for the values (beginning at right) $E/b = 2.5$ to 9.5 GeV by step of 1. The highlighted curve corresponds to the value $E/b = 6.5 \text{ GeV}$ which is the local intrinsic energy content of the

hadronizing QGP reball formed at SPS Pb{Pb interactions at the projectile energy 160A GeV. Dotted line, in figure 5, corresponds to $P = 0$, the solid line that follows it is the phase transition line where the QGP pressure is balanced by pressure of the hadron gas. This is the condition at which the equilibrium transition would occur in a slowly evolving system, such as would be the early universe. The properties of hadronic gas are obtained resum- ing numerically the contribution of all known hadronic particles including resonances, which effectively accounts for the presence of interactions in the confined hadron gas phase [16].

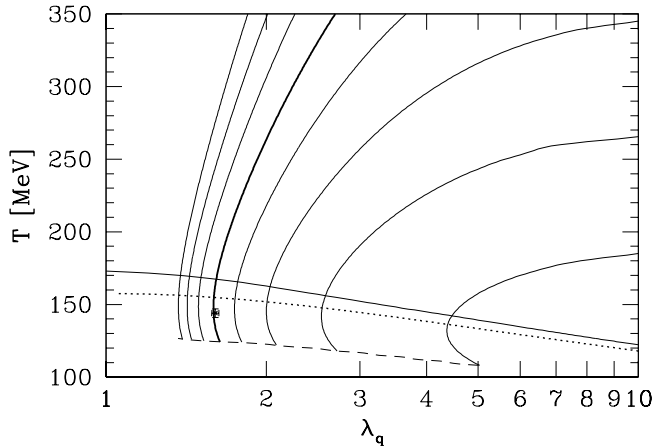


FIG. 5. Energy per baryon in QGP in the $T\{\lambda_q$ plane: >From right to left $E=b = 2.5$ to 9.5 GeV by step of 1, $E=b = 6.5$ GeV is highlighted. Dotted line corresponds to $P = 0$, above this the solid line is the phase transition where the QGP pressure is balanced by pressure of the hadron gas. The experimental point denotes chemical freeze-out analysis result [3], see section V. Bottom dashed line boundary is at energy density $0.5 \text{ GeV}/\text{fm}^3$.

One of the interesting quantities is the QGP energy density which we show in figure 6, for both fixed $E=b$ (top) and fixed $S=b$ bottom. We see that for $E=b > 6$ GeV and $S=b > 25$ the influence of finite baryochemical potential is minimal and the lines coalesce. In other words, at conditions we encounter at SPS, we can correlate the energy density with temperature alone. These results were obtained with $n_f = 2.5$ and thus apply to a fully quark-chemically equilibrated plasma state, and thus one should use these results primarily to explore the behavior of energy density in the late stages of plasma reball evolution. We see, in figure 6, that the energy density $3 \text{ GeV}/\text{fm}^3$ is established when the temperature in the reball equals 212 MeV . This occurs without any doubt in history of the QGP reball considering the high inverse slopes of particles observed. Our evaluation of the properties of the QGP liquid is at this temperature $T \approx 1.5T_c$ reliable.

As a final step in the study of the properties of the QGP liquid, we consider the conditions relevant for the

formation of the QGP, and consider the behavior for $n_f = 1$. We show, in figure 7, lines of fixed energy per baryon $E=b = 3, 4, 5, 6, 8, 10, 20, 50$ and 100 GeV, akin to results we have shown for $n_f = 2.5$, in figure 5. The horizontal line is where the equilibrated hadronic gas phase has the same pressure as QGP-liquid with semi-equilibrated quark abundance. The temperature of the QGP liquid must be higher to assure that hadrons have dissolved into the plasma phase. The dotted lines in figure 5, from bottom to top, show where the pressure of the semi-equilibrated QGP phase is equal to $\tau = 20\%, 40\%, 60\%, 80\%$ and 100% , being the 'stopping' fraction of the dynamical collisional pressure [17]:

$$P_{\text{col}} = \tau \frac{P_{\text{CM}}^2}{E_{\text{CM}}}$$

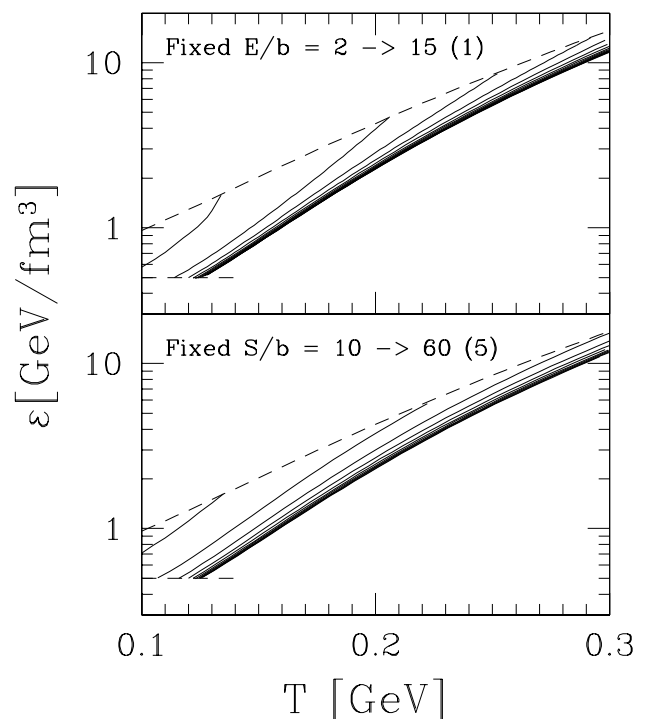


FIG. 6. Energy density in QGP as function of temperature. Top panel: for a fixed Energy per baryon $E=b = 2$ to 15 GeV by step of 1; bottom panel for fixed entropy per baryon $S=b = 10$ to 60 by step of 5. Boundaries are $\tau = 0.5 \text{ GeV}/\text{fm}^3$ at the bottom and $\tau = 1 \text{ GeV}$ at the top.

The rationale to study these lines is that, during the nuclear collision which lasts about $2R_N = \gamma_L 2c \tau' = 13 = 18 \text{ fm}/c$, where γ_L is the Lorentz factor between the lab and CM frame and R_N is the nuclear radius, parton collisions lead to a partial (assumed here to be $1/2$) chemical equilibration of the hadron matter. At that time, the pressure exercised corresponds to collisional pressure P_{col} . This stopping fraction, seen in the transverse energy produced, is about 40% for S{S collisions at 200 A GeV and 60% for Pb{Pb collisions at 158 A GeV . If the

momentum-energy and baryon number stopping are similar, as we see in the experimental data, then the SPS collisions at 160{200A GeV are found in the highlighted area left of center of the figure. In the upper right corner of this area we would expect the beginning evolution of the Pb{Pb reball and in the lower left corner of the S{S reball. We note that the temperature reached in S{S case is some 25 MeV lower than in the Pb-Pb case.

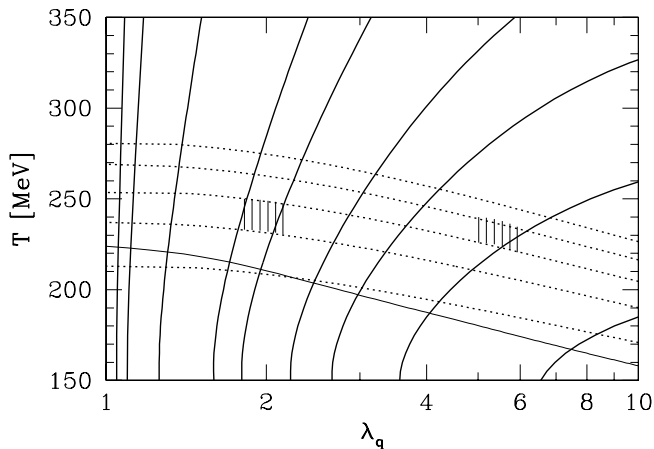


FIG .7. Energy per baryon in QGP in the T vs λ_q plane for $n_f = 1$: From right to left $E = 3, 4, 5, 6, 8, 10, 20, 50$ and 100 GeV . Thin, nearly horizontal line: hadronic gas phase has the same pressure as the QGP-liquid with semi-equilibrated quark flavor. Dotted lines from bottom to top: pressure in QGP liquid equals 20% ,40% ,60% ,80% , and 100% , of the dynamical collisional pressure

The highlighted area, right of center of the figure 7, corresponds to the expected conditions in Pb{Pb collisions at 40A GeV . If we assume that the stopping here is near 80% , then the initial conditions for reball evolution would be found towards the upper right corner of this highlighted area. We recognize that the higher stopping nearly completely compensates the effect of reduced available energy in the collision and indeed, we expect that we form QGP also at these collision energies. However, it is important to realize that we are entering a domain of parameters, in particular λ_q , for which the extrapolation of the lattice results is not necessarily reliable.

The case study $n_f = 1$ we presented is motivated by the finding that chemical equilibration of quarks is occurring slower than the chemical equilibration of gluons. The chemical relaxation time constant for the production of light quarks has been already obtained in the first consideration of chemical QGP equilibration, see figure 2 in [18]: $\tau_{GG \rightarrow qq} (T = 250 \text{ MeV}) = 0.3 \text{ fm}$. However, this calculation assumed that gluons were present in chemical equilibrium . Since gluon fusion processes are proportional to the square of gluon abundance, this value becomes 1.2 fm for processes occurring when gluons are at

50% of equilibrium abundance. This slow quark relaxation explains why quarks trail gluons in the approach to equilibrium . However, the value of n_f could be yet smaller than what we assumed. Thus we explore, in figure 8, the change of both the initial temperature T_i (upper panel) and λ_q (lower panel) as function of n_f for $E = 8 \text{ GeV}$, the case of Pb{Pb collisions at CERN . We see that, in the initial state, an equilibrated glue phase at $T = 260\{270 \text{ MeV}$ may have been reached.

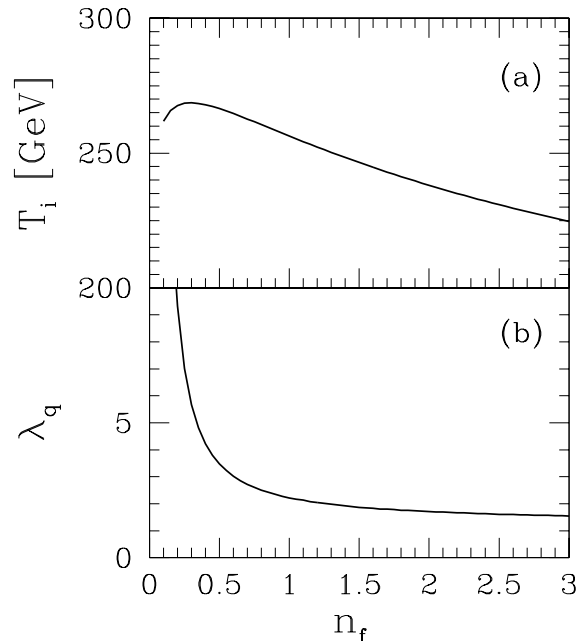


FIG .8. The initial conditions as function of the number of Fermi degrees of freedom n_f . Upper panel for temperature and lower for quark fugacity, at $E = 8 \text{ GeV}$.

V . EXPERIMENTAL DATA ANALYSIS AND QGP-EOS

A full account of our prior analysis of the 158A GeV Pb{Pb collision system has appeared [3,4]. We briefly summarize the results that we require for the study of QGP properties at reball breakup. In table I, in upper section, we present the parameters T_f (the chemical freeze-out temperature), v_c (the collective flow velocity at sudden breakup), λ_q (the light quark fugacity), λ_s (the strange quark fugacity), λ_q (the light quark phase space occupancy), λ_s (the strange quark phase space occupancy). These are derived from analysis of all hadrons excluding \bar{K} and \bar{K}^* , which data points are not following the same systematic production pattern. These parameters characterize completely the physical properties of the produced hadrons, and these properties are shown in the bottom section of table I.

In the heading of the table, the total error, σ is shown, along with the number of data points N , parameters p and data point constraints r . The confidence level that is reached in our description is near or above 90% , depend-

ing on scenario considered. The scenarios we consider are seen in the columns of table I: an unconstrained description of all data in the first column, constrained to exact strangeness conservation in the observed hadrons, second column. Since in both cases the parameter q assumes value that maximizes the entropy and energy content in the pion gas, we assume this value in the so constrained third column.

Given that progress we have reached in the study of QGP equations of state, we can now check the consistency between the statistical parameters (top panel of table I) and the physical properties of the reball (bottom panel of table I) which are maintained in the process of hadronization. We must remember that the energy, shown in this table, is the CM-laboratory energy which includes the low Lorentz factor $\gamma = 1.1$ $v_c^2 = 1.19$. Thus, the intrinsic thermal value of $E_{i=B}$ that we need to compare with using EoS of QGP, is $E_{i=B} = 6.5 - 0.4 \text{ GeV}$. This value, at temperature $T_f = 143 - 4 \text{ MeV}$ is shown in bottom panel in figure EOSS x where it falls right on the $S=B = 40$ curve, which is 5% below the entropy value seen in hadrons, $S_f=B = 42 - 3$. Similarly, the baryochemical potential $\mu_b = 3T_f \ln q$ we find is as required for the point on the top panel in figure 4 to appear right at the $S=B = 40$ line. A similarly embarrassing agreement of the hadron yield analysis results with properties of the QGP liquid reball is seen in figure 5, but that is just a different representation (at fixed $E_{i=B}$) of the result we saw at fixed $S=B$, in figure 4. However, the importance of this result is that the plasma breakup point appears well below the phase transition temperature line (thin horizontal solid line).

TABLE I. Results of study of Pb{Pb hadron production [3]: in the heading: the total quadratic relative error $\frac{\sigma}{T}$, number of data points N , parameters p and redundancies r ; in the upper section: statistical model parameters which best describe the experimental results for Pb{Pb data. Bottom section: specific energy, entropy, anti-strangeness, net strangeness of the full hadron phase space characterized by these statistical parameters. In column one, all statistical parameters and the low vary. In column two we χ_s by requirement of strangeness conservation, and in column three, we χ_q at the pion condensation point $q = \frac{c}{q}$.

	Pb j		Pb $\frac{eb}{f}$		Pb $\frac{fc}{f}$	
$\frac{\sigma}{T}; N; p; r$	2.5; 12; 6; 2		3.2; 12; 5; 2		2.6; 12; 5; 2	
T_f [MeV]	142	3	144	2	142	2
v_c	0.54	0.04	0.54	0.025	0.54	0.025
q	1.61	0.02	1.605	0.025	1.615	0.025
s	1.09	0.02	1.10		1.09	0.02
q	1.7	0.5	1.8	0.2	$\frac{c}{q} = e^{\mu_b = 2T_f}$	
$s = q$	0.79	0.05	0.80	0.05	0.79	0.05
$E_f=B$	7.8	0.5	7.7	0.5	7.8	0.5
$S_f=B$	42	3	41	3	43	3
$S_f=B$	0.69	0.04	0.67	0.05	0.70	0.05
$(S_f \quad S_f)=B$	0.03	0.04	0		0.04	0.05

For a vanishing baryochemical potential, $q = 1$, we determine in figure 5, that the phase transition temperature is $T_p = 173 \text{ MeV}$. The super-cooled $P = 0$ temperature is at $T_c = 157.5 \text{ MeV}$ (dotted line at $q = 1$ in figure 5), and an expanding reball can super-cool to as low as $T = 140 \text{ MeV}$, where the mechanical instability occurs [5].

The collective velocity v_c of the exploding matter is at this point expected to be large. v_c enters the definition of the local thermal energy as discussed in above paragraph, and thus the agreement with the data verifies the magnitude of v_c as determined. Interestingly, our central value $v_c = 0.54$ is the velocity of sound of the exploding reball:

$$v_s^2 = \frac{\partial P}{\partial \epsilon} \Big|_{S=B} \quad (13)$$

The theoretical line shown in figure 9, is at $S=B = 40$.

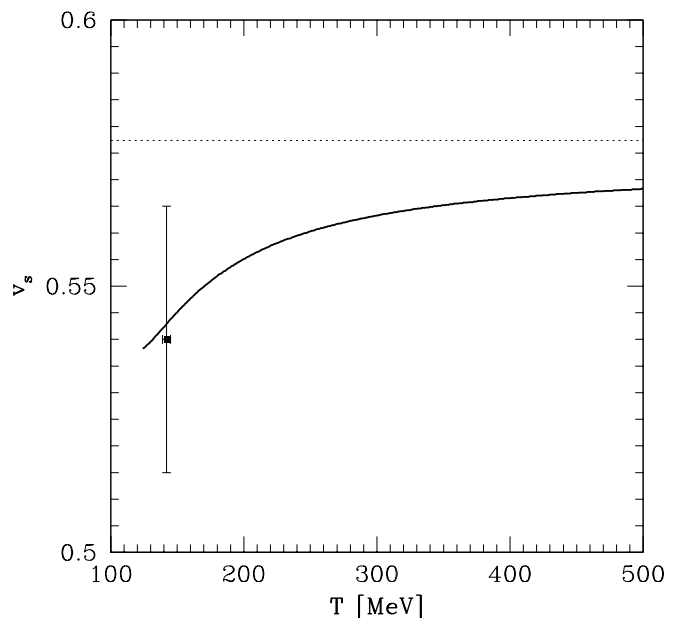


FIG. 9. The velocity of sound of quark-gluon liquid at $S=B = 40$. The dotted line corresponds to the value of the sound velocity of an ideal relativistic gas, $v_s = 1/\sqrt{3}$.

It is clear, from this discussion, that the properties of the QGP liquid at point of hadronization are just what we found studying the properties of hadrons emerging from the exploding reball. Both the specific energy and entropy content of the reball are consistent with the statistical parameters T_f and μ_b according to our equations of state of the quark-gluon liquid, and there is evidence that the low velocity seen in the data is near to velocity of sound.

There is yet more evidence for the QGP nature of the reball. We have discussed before that the values of the three other chemical parameters, $s; q$ and s , suggest as source a deconfined QGP reball [3].

a) The value of strange quark fugacity λ_s can be obtained from the requirement that strangeness balances, $\ln N_s - N_{s,i} = 0$; which for a source in which all s and \bar{s} quarks are unbound and thus have symmetric phase space, implies $\lambda_s = 1$. However, the Coulomb distortion of the strange quark phase space plays an important role in the understanding of this constraint for Pb{Pb collisions, leading to the Coulomb-deformed value $\lambda_s \approx 1.1$, which is identical to the value obtained from experimental data analysis $\lambda_s = 1.09 \pm 0.02$.

b) The phase space occupancy of light quarks λ_q is, before gluon fragmentation, near or at the equilibrium value $\lambda_q = 1$. However, as measured by hadron abundances, it is expected to significantly exceed unity to accommodate the contribution from gluon fragmentation into light quark pairs. There is an upper limit: $\lambda_q < \frac{c}{q} e^{m_c/2T_f} \approx 1.67$, which arises to maximize the entropy density in the confined hadron phase.

c) The strange quark phase space occupancy λ_s can be computed within the framework of kinetic theory, and is mainly influenced by strangeness pair production in gluon fusion [18], in early stages of the collision at high temperature, and by dilution effect in which the already produced strangeness oversaturates the 'thinner' low temperature phase space. Moreover, some gluon fragmentation also enriches λ_s as measured by hadron abundance. We note that some other groups implicitly address the parameter $\lambda_s = \lambda_q$ which therefore is stated in table I.

It is furthermore worthwhile to recall that the strangeness yield, $s = b \approx 0.7$, predicted early on as the result of QGP formation [18], was found in our data analysis, and is highly consistent with QGP assumption [3].

The results of our data analysis, shown in table I, have been controversial, mainly since the chemical freeze-out temperature T_f seemed to be too low, considering that the phase transition temperature has been estimated at 170 MeV. However, we now have shown, see figure 5, that the low value $T_f = 143$ MeV is due to deep supercooling of the rapidly expanding QGP, and there is a good agreement of our findings about the phase transition in an equilibrium system with the consensus view. It is important to stress that in the non-equilibrium data analysis approach, the precision we reach describing hadronic particle production other than π and K is very high. Thus we believe that with the understanding of supercooling this controversy will be settled.

Because of the high precision we reach in our data analysis, we noted that the experimental abundance of π and K particles is above the yield pattern established by other strange hadrons. The π excess we found is only 1.5 s.d.. However, the K excess is 5 s.d. and thus it seems that another production mechanism contributes to this yield, beyond a purely statistical QGP fragmentation-recombination model. Forcing light quark equilibrium yields higher T_f which reduces excess, but the high value of total theory (experiment discrepancy) implies that some essential physical element is missing. When seeking to resolve this, we in fact have found that

the light quark pair abundance nonequilibrium and an additional production mechanism are required.

V I. D I S C U S S I O N A N D C O N C L U S I O N S

We have presented a detailed study of the interacting quark-gluon plasma equations of state, which have the property to reproduce precisely the latest lattice results for pressure and energy density. Since lattice results are obtained at vanishing baryon density, we must rely on theoretical behavior of the interacting quark-gluon gas when considering finite baryon density. This is done within the same computational approach in which the pressure and energy density are obtained correctly. Moreover, it turns out that the interaction correction is smallest for the baryon density, and thus, a priori, is most reliably described; however its magnitude increases to the level of 45% at phase boundary. We also extrapolated to finite baryon density the interaction scale μ , as given in Eq. (3). Since there is arbitrariness of this extrapolation, we did check that, in the region of interest in the discussion of the SPS experimental data, the detail how the baryochemical potential is introduced into interaction scale does not matter: μ -contribution is in fact completely dominated by T -contribution, since $(T_c)^2 \approx 50 \frac{q}{q}$.

We have shown that the initial state of the QGP rebal, in pre-chemical equilibrium stage of light quarks, has been formed at about $T \approx 250$ MeV, see figure 7. By the time, light quarks equilibrate temperature drops to just above $T \approx 210$ MeV, and the energy density in such a QGP rebal is at 3 GeV/fm³, as can be seen in figure 6, following the $S = b \approx 0.42$ constrain back in time towards high temperature. The freeze-out point at $T \approx 143$ MeV, seen in bottom panel of figure 4, corresponds to an energy density $\mu_f \approx 0.6$ GeV/fm³. This is the value for the supercooled plasma, the equilibrium phase transition occurs at twice this value, $\mu_p \approx 1.2$ GeV/fm³.

A significant change in the reaction mechanism can be expected when the opacity of the colliding nuclei is at or below 20%. Inspecting figure 7, we see that at that point, formation of a deconfined phase is not assured considering where the boundary between hadrons and chemically non-equilibrated QGP is seen. This transparency certainly occurs for sufficiently small systems, where small is smaller than $S \{S$, where stopping at the level of 35% is observed. On the other hand, results shown in figure 7 strongly suggest that the QGP-liquid phase should be formed at all energies accessible to SPS for Pb{Pb collisions. In fact, were it not for the uncertainties of extrapolation of lattice results to high baryon density, we would be rather certain that deconfinement also occurs in AGS energy range.

The results presented here confirm in quantitative terms that the earlier nonequilibrium analysis of hadron production is valid [3]. The non-equilibrium analysis

method is more general than the equilibrium models, and it describes the hadron production data much better than competing approaches which assume quark chemical equilibrium conditions. Then why is not everybody using our approach? It is very hard to find a good answer to this question also posed by Biro [6]. On the other hand, experimental results are to help reach a decision. Is there evidence for chemical non-equilibrium, that is for $\mu_q > 1$, or alternatively for $T_f < 160$ MeV today?

a) We have studied pion spectra and have shown how these depend on chemical non-equilibrium [19]. We have found that soft pion data, in fact, qualitatively behave in way expected for a large value of μ_q . It is difficult to extract relevant information from HBT studies of pion correlations.

b) We have here undertaken the precise study of the QGP-EoS in order to check if the low chemical freeze-out temperature we find, $T_f \approx 143$ MeV, is in fact consistent with the QGP hypothesis for the rebal. As discussed in section V, we obtained an astounding agreement between the QGP rebal properties and our earlier analysis of hadron production experimental results.

In conclusion, we have shown that equations of state of the quark-gluon liquid, fine tuned to exactly agree with the lattice results [2], are allowing a straightforward interpretation of the observed properties of the hadron rebal. We found that the energy per baryon and the entropy per baryon are agreeing with results of hadron production analysis, and that the velocity of expansion has the right magnitude and as determined in data analysis is just the sound velocity. The important point is that the quark-gluon liquid properties are found to be consistent with the observed physical properties of the rebal of dense hadronic matter formed in 158A GeV central Pb{Pb interactions at CERN.

It is important for the reader to appreciate that we did not fit any property of QGP, and that our comparison is based on EoS directly derived and extrapolated from the lattice-QCD results, using established expressions of thermal field theory. The only uncertain extrapolation, as it is not based on lattice data, is that we use for the baryon density a purely theoretical result which, however, is obtained by the same method as the pressure and energy (and entropy) which agrees with the lattice result once the two parameters, the scale (T) and vacuum energy B , are fixed.

In our judgment, the good agreement we find between hadron abundance analysis and properties of lattice-EoS leave little if any doubt that the SPS experiments involving Pb{Pb collisions at 158A GeV have reached the quark-gluon plasma phase of hadronic matter.

Supported in part by a grant from the U.S. Department of Energy, DE-FG 03-95ER 40937.

LPTHE, Univ. Paris 6 et 7 is: Unité mixte de Recherche du CNRS, UMR 7589.

- [1] <http://www.cern.ch/CERN/Announcements/2000/NewStateMatter>. Text of the scientific consensus view of the spokesman of CERN experiments also available as: nucl-th/0002042, "Evidence for a New State of Matter: An Assessment of the Results from the CERN Lead Beam Program meeting", compilation by U. Heinz and M. Jacob
- [2] F. Karsch, E. Laermann and A. Peikert, Phys. Lett. B 478, 447-455, (2000).
- [3] J. Letessier and J. Rafelski, "Observing Quark-Gluon Plasma with Strange Hadrons", nucl-th/0003014, Int. J. Mod. Phys. E (2000) in press;
- [4] J. Letessier and J. Rafelski, Acta Phys. Pol. B 30, 3559 (1999).
- [5] T. Csorgo, and L.P. Csernai, Phys. Lett. B 333, 494 (1994).
- [6] T.S. Biro, "Quark Coalescence and Hadronic Equilibrium", hep-ph/0005067.
- [7] J. Letessier, A. Tounsi and J. Rafelski, Phys. Lett. B 389, 586 (1996).
- [8] S. Hamieh, J. Letessier, J. Rafelski, M. Schroedter and A. Tounsi, "Free Energy of a Hot Quark-Gluon Plasma", hep-ph/0004016.
- [9] P. Arnold and C. Zhai, Phys. Rev. D 50, 7603 (1994); 51, 1906 (1995).
- [10] C. Zhai and B. Kastening, Phys. Rev. D 52, 7232 (1995).
- [11] E. Braaten and A. Nieto, Phys. Rev. Lett. 76, 1417, (1996); and Phys. Rev. D 53, 3421 (1996).
- [12] J. Andersen, E. Braaten and M. Strickland, Phys. Rev. Lett. 83, 2139, (1999); Phys. Rev. D 61, 074016, (2000).
- [13] A. Peshier, B. Kampfer and G. So, Phys. Rev. C 61, 45203, (2000).
- [14] H. Vija and M.H. Thoma, Phys. Lett. B 342, 212, (1995).
- [15] S.A. Chin, Phys. Lett. B, 78, 552, (1978).
- [16] R. Hagedorn, Suppl. Nuovo Cimento 3, 147 (1965); R. Hagedorn, Cargèse lectures in Physics, Vol. 6, Gordon and Breach (New York 1977) and references therein; see also J. Letessier, H. Gutbrod and J. Rafelski, Hot Hadronic Matter, Plenum Press NATO-ASI series B 346, New York (1995); H. Grote, R. Hagedorn and J. Ranft, "Atlas of Particle Production Spectra", CERN black report (December 1970).
- [17] J. Rafelski, J. Letessier and A. Tounsi, Acta Phys. Pol. B 27, 1035 (1996), and references therein.
- [18] J. Rafelski and B. Müller, Phys. Rev. Lett. 48, 1066 (1982); and 56, 2334 (1986).
- [19] J. Letessier, A. Tounsi and J. Rafelski, Phys. Lett. B 475, 213 (2000).